



Hydrothermal Synthesis and Characterization of Tin Oxide (SnO₂) Nanoparticles

T. Regin Das^{1*}, M. Meena³, I. Vetha Potheher⁴, P. Aji Udhaya²

¹Department of Physics, Lekshmipuram Arts and Science College, Nagercoil, TN, India

²Department of Physics, S.T. Hindu College, Nagercoil, TN, India

³Department of Physics, Bharathidasan Institute of Technology, Anna University, BIT Campus, Tiruchy, TN, India

⁴Department of Physics, S.T. Hindu College, Nagercoil, TN, India

Received: 12.01.2020 Accepted: 22.02.2020

*regindphycis@gmail.com

ABSTRACT

Metal oxide nanoparticles have potential applications in a wide range of fields like medicinal and Environmental science. Tin Oxide (SnO₂) has been applied as a semiconductor nanomaterial in electronics. Tin oxide is a widely used and intensively studied n-type semiconductor. The research on tin oxide semiconductors has been growing due to the wide range of applications, especially as photo sensors, catalysts, and antistatic coating. The electrical conductivity and luminescence properties of SnO₂ are mainly decided by the oxygen vacancy present in it. This study intended to synthesize Tin Oxide (SnO₂) nanoparticles via a one-step hydrothermal method and study the effect of annealing temperature on its properties. As prepared, samples were annealed at two different temperatures, and the samples were characterized by Powder X-Ray Diffraction (PXRD), Ultra Violet – Diffusion Reflectance Spectroscopy (UV-DRS), and Photo Luminescence (PL). The dependence of Structural and optical properties with temperature was discussed.

Keywords: Oxide; Annealing Temperature; PXRD; UV-DRS; PL.

1. INTRODUCTION

Nanoparticle plays a significant role in research and development of the device, systems, and Structures in numerous areas. Tin Oxide is one of the most important materials due to its high degree of transparency in the visible spectrum, strong, physical, and chemical interaction with adsorbed species, low operating temperature, and strong thermal stability in the air up to 500 °C (Rahman *et al.* 2010). Tin Oxide (SnO₂) is classified as a II-VI composite semiconductor based on its group II and VI periodic table components with 3.60 eV and 3.75 eV direct and indirect energy band gaps (Jain and Kumar, 2004). SnO₂ nanoparticles preparation can be achieved using several different techniques. These include the co-precipitation (Arularasu *et al.* 2018) Sol gel (Gu *et al.* 2004), Solvothermal decomposition (Davar *et al.* 2010), microwave hydrothermal synthesis (Ponzoni *et al.* 2015), and precipitation (Gaber *et al.* 2014) techniques. However, issues related to the complexity of the synthetic process include the creation of a pure by-product, reagent toxicity, and longer reaction times, which have made industrial SnO₂ nanoparticle generation challenging to achieve (Tran *et al.* 2017).

It is essential to have inexpensive methods for obtaining nanoparticles with no special atmosphere and high temperature. The hydrothermal method is a suitable chemical method in nanoparticle synthesis because it does not require high pressure and high temperature, and

impurities are removed by filtration and washing. Tin presents in two oxidation states. Therefore two types of oxides are possible: Stannous oxide (SnO-romarchite) and Stannic Oxide (SnO₂- Cassiterite) (Vila and Rodriguez – Paez, 2009) SnO₂ is an n-type semiconductor and is more stable than SnO. It is widely used in Optoelectronic devices (He *et al.* 2006), Electrodes for Lithium-ion batteries (He *et al.* 2005), solar cells (Ge *et al.* 2006), Transistors, and gas sensors to detect combustible gases such as H₂S, CO, Liquid petroleum, NO₂ and C₂H₅OH (Hwang and Choi, 2009).

The surface to volume ratio (S/V) of SnO₂ nanoparticles is high compared to the bulk tin oxide, which results in increased sensitivity and adsorption. The electrical conductivity and luminescence properties of SnO₂ are mainly decided by the oxygen vacancy present in SnO₂ lattice (Gu *et al.* Wang, 2004), and they are also affected by surface to volume (S/V) ratio. In this report, the particle size and lattice parameters were analyzed using XRD for SnO₂ nanoparticles, bandgap and photoluminescence were measured using UV and PL studies for unannealed SnO₂ and annealed at 100 °C and 600 °C.

2. EXPERIMENTAL PROCEDURE

The materials used for the preparation of SnO₂ Nanoparticle are dihydrated Stannous Chloride (SnCl₂.2H₂O), urea (CH₄N₂O), and Sodium Hydroxide

(NaOH) Pellets. The calculated amount of stannous chloride was dissolved in 100 ml of pure distilled water as the starting solution. The calculated amount of urea solution was also prepared separately by dissolving urea in 100 ml of distilled water. Then the solutions were mixed and stirred well for about 15 minutes. During the time of stirring NaOH solution was added drop by drop such that it attains a suitable pH value. The resultant solution is then stirred for 15 minutes using magnetic stir. The light milky colored solution obtained was then changed to Borosil Pot and placed into a microwave oven. The oven was operated for 30 minutes at medium temperature.

After cooling, the product obtained was then washed with distilled water and Benzene. Then, it was filtered using wattman filter paper and dried at room temperature. Parts of the prepared samples were then annealed at 100 °C and 600 °C for two hours in the heating furnace.

The structural behavior of as-prepared and annealed SnO₂ was characterized by XRD analysis with X-Ray wavelength – 1.5406 Å and scanning range of 3 to 80 degrees. The mean crystallite size (D) of the nanoparticles were estimated using the Debye-Scherrer formula as,

$$D = 0.9\lambda / \beta \cos\theta$$

Where λ , β , and θ are the X-ray wavelength (1.5406Å°).

The full-width Half maximum (FWHM) of diffraction peak and diffraction angle, respectively. Bradley-Joy and Nelson - Rilay graph also drawn to the samples to get the corrected value of the lattice parameter.

3. RESULT & DISCUSSION

3.1 X-ray diffraction analysis

All the synthesized samples were characterized for their Crystal structure, Particle size, and lattice parameters. The XRD pattern of prepared SnO₂ is given in fig1. It shows a crystalline phase with broad diffraction peaks corresponding to a tetragonal structure. All the peaks of the XRD belongs to the tetragonal lattice of SnO₂ coincide with the tetragonal structure of SnO₂ in JCPDS file (File No;88-0287). The lattice parameters are calculated using unit cell software (Method of TJB Holland & SAT Redform 1995).

The spacing between diffracting planes (d) of SnO₂ was calculated by Bragg equation $2d\sin\theta = n\lambda$ and the lattice parameters ($a=b\neq c$) for tetragonal phase structure was determined by the equation

$$1/d = (h^2 + k^2)/a^2 + l^2/c^2$$

The calculated values of a, c, and cell volumes are given in Table1. The increase of annealing temperature from 100 °C to 600 °C shows no significant variation in the lattice parameter and cell volume that was the dehydroxylation of the material due to the presence of some hydroxyl group in the Tin Oxide crystallites annealed at 100 °C, which generates a non-perfect rutile structure, the samples annealed at higher temperature showed the perfect rutile structure (Antonio *et al.* 2003). The narrowness of the peaks towards the increased annealing temperature indicating that the SnO₂ nanoparticles crystallize as the temperature increases.

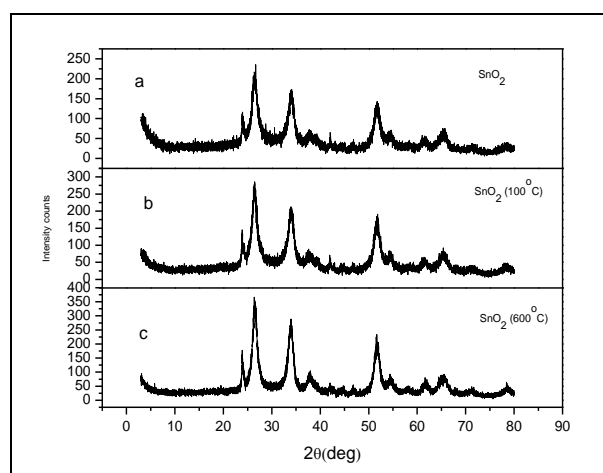


Fig. 1: XRD Pattern of SnO₂ (a) Un Annealed (b) Annealed at 100 °C (c) Annealed at 600°C

The crystallite size of the SnO₂ nanoparticles measured using the Scherrer formula is 5.17, 6.32, and 6.43 nanometers for unannealed SnO₂, annealed at 100 °C and 600 °C, respectively. Fig2 is the Williamson-Hall plot drawn between $4\sin\theta$ and $\beta\cos\theta$. The intercept of $\beta\cos\theta$ value at Y-axis gives $0.9\lambda/D$ from which the particle size D was calculated, and the slope of the line gives the lattice strain ($C\epsilon$).

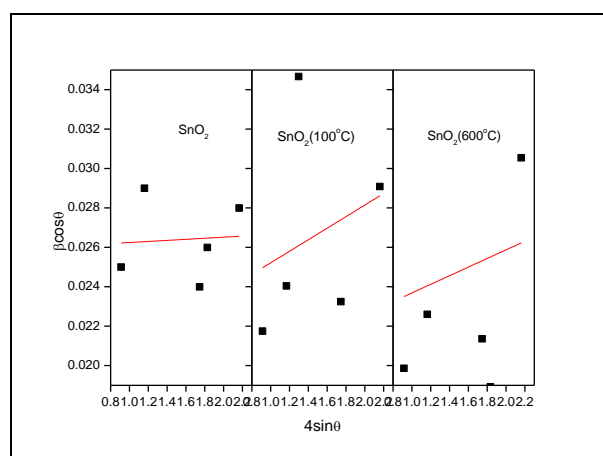


Fig. 2: Williamson-Hall Plot of SnO₂ Annealed at Different Temperatures

Table 1. Cell Parameters and Cell Volume of SnO₂

| Sample | a | c | Cell Volume |
|-------------------------------------|------|------|-------------|
| SnO ₂ -Unannealed | 4.76 | 3.17 | 71.97 |
| SnO ₂ -Annealed at 100°C | 4.77 | 3.17 | 72.12 |
| SnO ₂ -Annealed at 600°C | 4.76 | 3.19 | 72.29 |

From Table 1 & 2 it was observed that the strain value decreased and particle size increased as the annealing temperature is increased.

Table 2. The Intercept and Slope of Williamson-Hall Plot for SnO₂

| Sample | Unannealed - SnO ₂ | SnO ₂ - Annealed at 100 °C | SnO ₂ - Annealed at 600 °C |
|--------------------|-------------------------------|---------------------------------------|---------------------------------------|
| Intercept | 0.019 | 0.022 | 0.020 |
| Slope (strain) | 0.006 | 0.003 | 0.002 |
| Particle size (nm) | 5.17 | 6.32 | 6.43 |

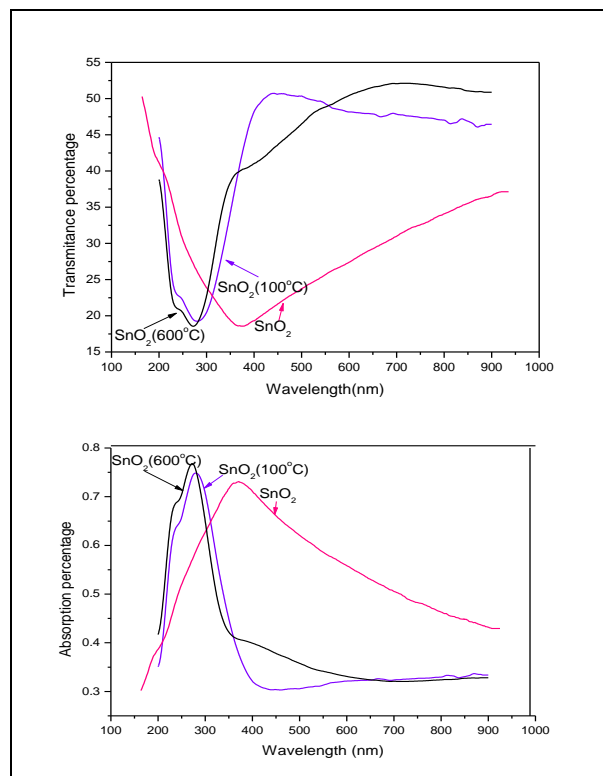
3.2 UV-DRS-Analysis

In order to study the effect of annealing on optical properties of SnO₂ nanoparticles, UV-diffuse reflectance measurements were carried out. Fig3 shows the recorded UV spectra of the prepared unannealed samples and samples annealed at 100°C and 600°C.

The diffuse reflectance spectra studies are more important to estimate the optical bandgap of the materials. The calculated band gap for unannealed SnO₂ nanoparticles and particles annealed at 100°C and 600°C were found to be 3.744 eV, 3.60eV, and 3.21eV, respectively. Our current study shows that, As the annealing temperature increases, the bandgap energy decreases. It is suggested that the decrease in bandgap could be due to transitions between Sn²⁺ ion d-shell electrons' valance and conduction bands (Choi et al. 1996). Given this, it is difficult to eradicate the particle size effect on the bandgap.

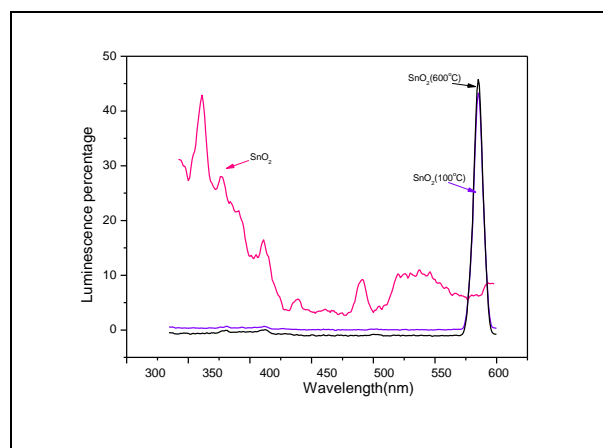
It is possible to change the band structure and material attributes due to the reduction in the particle size with a reduction in the bandgap, similarly resulting in greater particle size. Thus, smaller particle sizes can be associated with overlap with s-electron and p-electron conduction bands separating in higher energy conditions. Higher calcination temperatures were associated with lower bandgap values. It is suggested that the temperature rise may cause an incremental increase in the absorption coefficient because of an increase of defected states. Electron-hole pairs are produced through photon absorption, generating a field that could change the

optical attributes and electronic structure of nanoparticle products.

**Fig. 3: Absorption and Transmittance spectra of SnO₂ annealed at different temperatures.**

3.3 Photoluminescence Study

Besides the size quantization, surface effects are also known to influence the optical properties of these nanometer particles. It has been shown recently that the photoluminescence emission of the nanocrystals is sensitive to the presence of defects that might arise because not all the dangling bonds on the particle surface can be saturated by molecular legends (yang *et al.* 1996).

**Fig. 4: Photoluminescence Spectra of SnO₂ Nanoparticles Annealed at Different Temperatures**

In the present study, photoluminescence emission spectra were recorded in the wavelength range 300 to 600 nm for the excitation at 585 nm. Fig4 shows the recorded photoluminescence spectra of the SnO₂ nanoparticles annealed at various temperatures 100 °C and 600 °C.

4. CONCLUSION

The results of this study demonstrate the effect of annealing on particle size. The nanoparticles were synthesized without the requirement of any special atmosphere and pressure. This study provides an inexpensive and easy method to prepare and improve the quality of SnO₂ nanoparticles. Less particle size was obtained at the lower annealing temperature. The optical studies show that band gap variation is also achieved by varying the annealing temperature corresponding to the particle size.

REFERENCES

- Arai, T., The study of the optical properties of conducting tin oxide films and their interpretation in terms of a tentative band scheme, *J. Phys. Soc. Jpn.*, 15, 916–927(1960).
<https://doi.org/10.1143/JPSJ.15.916>
- Arularasu, M., Anbarasu, M., Poovaragan, S., Sundaram, R., Kanimozhi, K., Magdala, C. M., Kaviyarasu, K., Thema, F. T., Letsholathebe, D., Mola, G. T. and Maaza, M., *J. Nanosci. Nanotechnol.*, 18(5), 3511–3517(2018).
<https://doi.org/10.1166/jnn.2018.14658>
- Avila, H. A. and Rodriguez-Paez, J. E., Solvent effects in the synthesis of tin oxide, *J. Non-Cryst. Solids.*, 355(14-15), 885-890(2009).
<https://doi.org/10.1016/j.jnoncrysol.2009.03.004>
- Choi, W. K., Jung, H. J. and Koh, S. K., Chemical shifts and optical properties of tin oxide films grown by a reactive ion assisted deposition, *J. Vac. Sci. Technol. A.*, 14, 359–366(1996).
<https://doi.org/10.1116/1.579901>
- Davar, F., Salavati-Niasari, M. and Fereshteh, Z., Synthesis and characterization of SnO₂ nanoparticles by thermal decomposition of new inorganic precursor, *J. Alloys Compd.*, 496(1-2), 638–643(2010).
<https://doi.org/10.1016/j.jallcom.2010.02.152>
- Gaber, A., Abdel-Rahim, M. A., Abdel-Latif, Y. A. and Abdel-Salam, M. N., Influence of calcination temperature on the structure and porosity of nanocrystalline SnO₂ synthesized by a conventional precipitation method, *J. Electrochem. Sci.*, 9, 81–95(2014).
- Ge, J. P., Wang, J., Zhang, H. X., Wang, X., Peng, Q. and Li, Y. D., High ethanol sensitive SnO₂ microspheres, *Sensor Actuat. B: Chem.*, 113(2), 937-943(2006).
<https://doi.org/10.1016/j.snb.2005.04.001>
- Gu, F., Wang, S. F., Lu, M. K., Zhou, G. J., Xu, D. and Yuan, D. R., Photoluminescence properties of SnO₂ nanoparticles synthesized by sol-gel method, *J. Phys. Chem. B.*, 108, 8119-8123(2004).
<https://doi.org/10.1021/jp036741e>
- Gu, F., Wang, S. F., Lü, M. K., Zhou, G. J., Xu, D. and Yuan, D. R., Photoluminescence properties of SnO₂ nanoparticles synthesized by sol-gel method, *J. Phys. Chem. B.*, 108, 8119–8123(2004).
<https://doi.org/10.1021/jp036741e>
- He, Jr. H., Wu, Te. H., Hsin, C. L., Li, K. M., Chen, L. J., Chueh, Y. L. and Wand, Z. L., Beaklike SnO₂ nanorods with strong photoluminescent and field-emission properties, *Small*, 2(1), 116-120(2005).
<https://doi.org/10.1002/sml.200500210>
- He, Z. Q., Li, X. H., Xion, L. Z., Wu, X. M., Xiao, Z. B. and Ma, M. Y., Wet chemical synthesis of tin oxide-based material for lithium ion battery anodes, *Mater. Res. Bull.*, 40(5), 861-868(2005).
<https://doi.org/10.1016/j.materresbull.2004.06.021>
- Hwang, I. S., Choi, J. K., Kim, S. J., Dong, K. Y., Kwon, J. H., Ju, B. K. and Lee, H. J., Enhanced H₂S sensing characteristics of SnO₂ nanowires functionalized with CuO, *Sensor. Actuat. B : Chem.*, 142(1), 105-110(2009).
<https://doi.org/10.1016/j.snb.2009.07.052>
- Jain, G. and Kumar, R., Electrical and optical properties of tin oxide and antimony doped tin oxide films, *Opt. Mater.*, 26(1), 27–31(2004).
<https://doi.org/10.1016/j.optmat.2003.12.006>
- Ponzoni, C., Cannio, M., Boccaccini, D., Bahl, C. R. H., Agersted, K. and Leonelli, C. S., Ultrafast microwave hydrothermal synthesis and characterization of Bi_{1-x}LaxFeO₃ micronized particles, *Mater. Chem. Phys.*, 162, 69–75(2015).
<https://doi.org/10.1016/j.matchemphys.2015.05.002>
- Rahman, N. A., Farrukh, M. A., J. Chin. Adnan R., Razana Chem. Soc.-Taip. (2010), 57, 22.
- Toledo - Antonio, J. A., Gutierrez-Baez, Sabastin, P. J. and Vazquez, A., Thermal stability and structural deformation of rutile SnO₂ nanoparticles, *J. Solid State Chem.*, 174, 241-248(2003).
[https://doi.org/10.1016/S0022-4596\(03\)00181-6](https://doi.org/10.1016/S0022-4596(03)00181-6)

Tran, V.-H., Ambade, R. B., Ambade, S. B., Lee, S.H.
and Lee, I. H., ACS Appl. Mater. Interfaces., 9(2),
1645–1653(2017).

<https://doi.org/10.1021/acsami.6b10857>